

calculation, where only individual atomic wave functions enter. This is in opposition to the more

complicated molecular-orbital computations necessary at small relative separation.

<sup>1</sup>F. London, *Z. Physik* **63**, 245 (1930).

<sup>2</sup>H. B. Levine and G. Birnbaum, *Phys. Rev.* **154**, 86 (1967), R. L. Matcha and R. K. Nesbet, *Phys. Rev.* **160**, 72 (1967).

<sup>3</sup>Z. J. Kiss and H. L. Welsh, *Phys. Rev. Letters* **2**, 166 (1959), D. R. Bosomworth and H. P. Gush, *Can. J. Phys.* **43**, 751 (1965).

<sup>4</sup>Retardation effects will only become significant when characteristic atomic wavelengths are smaller than the interatomic separation. For those transitions of the alkali atoms which possess large oscillator strengths the corresponding wavelengths exceed 1000 Å (e.g., the Na  $3s-3p$  transition). Thus, we might expect the present discussion to be applicable out to around 0.1- $\mu$  separation. (With some additional effort the present formalism may be extended to include the retardation effects.) On the other hand, the exchange contribution is of significance only when the wave functions overlap considerably. These wave functions decay exponentially with distance outside

the confines of the atom. Typical decay lengths can be found by examining the Bates-Damgaard approximate wave functions and are equal to  $(4\epsilon)^{-1/2}$ . For the alkali  $s$  states, this number lies between one and two atomic units. We have taken three decay lengths, or roughly five atomic units, as the point beyond which exchange may be neglected. We, therefore, regard  $Z$  as lying between 3 Å and 1000 Å.

<sup>5</sup>Y. M. Chan and A. Dalgarno, *Mol. Phys.* **9**, 349 (1965).

<sup>6</sup>C. L. Schwartz, *Ann. of Phys.* **2**, 170 (1959).

<sup>7</sup>J. O. Hirschfelder, C. F. Curtiss, and R. B. Bird, *Molecular Theory of Gases and Liquids* (John Wiley & Sons, Inc., New York, 1964). We have rewritten the expressions given by the above authors for the multipole interactions in spherical tensor form.

<sup>8</sup>F. Herman and S. Skillman, *Atomic Structure Calculation* (Prentice-Hall, Inc., Englewood Cliffs, New Jersey, 1963).

## Oxygen $K$ -Shell X-Ray Production in Thin Films of Aluminum Oxide by 20- to 100-keV Protons\*

R. R. Hart,<sup>†</sup> F. William Reuter, III, and Harold P. Smith, Jr.,  
*Space Sciences Laboratory and Department of Nuclear Engineering, University of California, Berkeley, California 94720*

and

J. M. Khan  
*University of California Lawrence Radiation Laboratory, Livermore, California*

(Received 4 October 1968)

The oxygen  $K$ -shell x-ray production cross section and the stopping power of aluminum oxide for 20- to 100-keV protons were determined by measurements of the oxygen  $K$  x-ray yield (x rays/proton) from surface films of aluminum oxide, formed on aluminum substrates by anodic oxidation. Ionization cross-section results are compared with previous measurements of C, Mg, and Al. The comparison shows that the cross sections follow the same trend, but depart from theoretical predictions based on the Born approximation. The stopping power data have maxima at proton energies of 65 and 90 keV, corresponding to peaks in the stopping powers of Al and O.

### INTRODUCTION

The interaction of protons of energy exceeding

1 keV is dominated by inelastic collisions between the proton and the atomic electrons of the medium. If an inner-shell electron is ejected from a target

atom, the subsequent filling of the vacancy may lead to the emission of a characteristic x ray.<sup>1</sup> The probability of such emission is determined by the production cross section for the electron shell considered. Since few cross sections of this type have been measured and since present theoretical descriptions based on the Born approximation fail at low proton energy,<sup>2</sup> the *K*-shell x-ray production cross section for oxygen was measured in the low energy range, 20 to 100 keV. The cross section was determined from measured oxygen *K* x-ray ( $O_K$ ) yields from thin,  $Al_2O_3$ , surface films of variable, but known, thickness which were formed by anodic oxidation of aluminum.

If the energy of the proton exceeds 1 MeV, the stopping power decreases with increasing proton energy. At lower energies, i. e., at proton velocities comparable to those of orbital electrons, sequential neutralization and ionization of the proton by capture and loss of orbital electrons dominates the interaction and, as a result the stopping power tends to peak at approximately 100 keV. It is in this energy range where little experimental data is available<sup>3</sup> and where the complications produced by electron capture and loss reduce the accuracy of theoretical descriptions.<sup>4</sup> The lack of data is largely a result of difficulty in obtaining sufficiently thin, self-supporting targets for transmission measurement. However, once the x-ray production cross section is determined, thick-target yield measurement then permits calculation of the stopping power. Hence, the aluminum oxide films were not self-supporting but were chemically bound to aluminum substrates. For comparison with previous work,<sup>2</sup> the aluminum *K* x-ray ( $Al_K$ ) yield for 40- to 100-keV protons incident on thick aluminum targets was also measured.

#### EXPERIMENTAL APPARATUS AND METHODS

The experimental apparatus has been described in detail in a previous publication.<sup>5</sup> The primary components are: (1) 100-keV proton ion source, (2) beam analyzing magnet, (3) ultrahigh-vacuum target chamber, and (4) gas proportional counter for detection of characteristic x rays. The counter was operated in flow mode (50 cc/min) utilizing methane at 50 Torr for  $O_K$  detection or *P*-10 gas (90% argon, 10% methane) at atmospheric pressure for  $Al_K$  detection. The counter windows were 4000 Å aluminum oxide or 0.0005-in. aluminum foil. The proportional counter pulses were discriminated by a single-channel pulse-height analyzer and counted by an electronic scaler, which was gated by a target current integrator.

Aluminum oxide surface films were formed on high purity (99.9999% Al), electropolished aluminum substrates by anodic oxidation at constant voltage for 10 min. The anodization voltage *V* (volts) was related to the oxygen surface density

*T* ( $\mu\text{g O/cm}^2$ ) of the thin films through the relationship<sup>5</sup>

$$T = (0.222)(V + 2.8). \quad (1)$$

The target surface normal was oriented  $45^\circ$  to the proton beam and to the direction of x-ray detection.

#### ALUMINUM *K* X-RAY MEASUREMENT

The  $Al_K$  yield from three electropolished, thick targets of aluminum bombarded by 40- to 100-keV protons were measured. The experimental observable, the number of x rays detected by the proportional counter per  $\mu\text{C}$  of incident protons, was corrected for solid angle attenuation and x-ray window absorption to give the x-ray yield. See Fig. 1. The measured deviation at any energy for our measurements is 6% and is composed of the deviation in x-ray counts (3%), integrated target current (1%), x-ray transmission (2%), and surface nonuniformity (5%). The last quantity was examined by observing x-ray yield at 100-keV proton energy as the target was rotated  $\pm 2^\circ$  about the target holder axis; thereby moving the beam spot  $\pm \frac{1}{8}$  in. on the target surface. It should be noted that the mean value of the yield at any energy is within 10% of the results reported by Khan *et al.*<sup>2</sup>

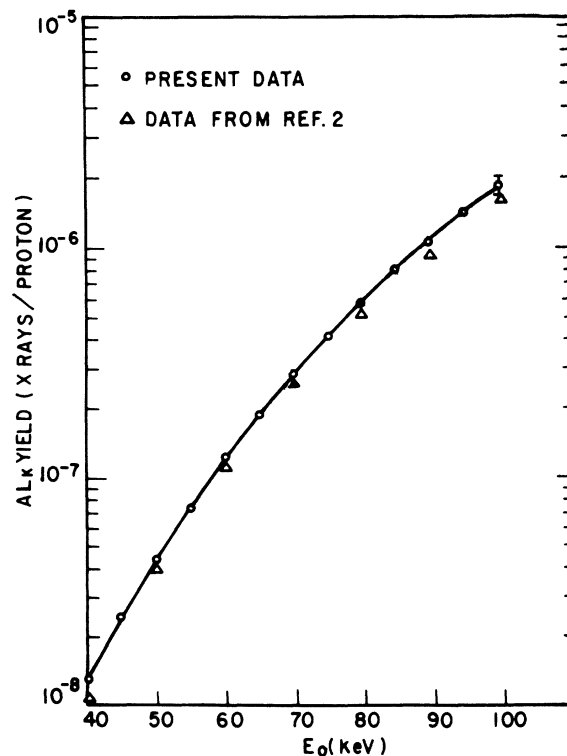


FIG. 1. Comparison of the  $Al_K$  yields from thick-target aluminum with the results from Ref. 2.

## OXYGEN K X-RAY MEASUREMENT

## Theory

Assuming straight proton trajectories, isotropic x-ray emission (experimentally verified in Ref. 1 for  $L$ -shell x-rays produced in a gold target), a uniform aluminum oxide film, and a mathematically plane target surface with surface normal oriented  $45^\circ$  with respect to the proton beam and to the direction of x-ray detection, the characteristic  $O_K$  x-ray yield,  $I$  (x rays/proton), is given by<sup>1</sup>

$$I(E_0, T) = n \int_0^T dx \sigma[E(E_0, x)] e^{-\mu_a x}, \quad (2)$$

where  $E_0$  is the initial proton energy,  $T$  the oxygen surface density in  $\mu\text{g}$  oxygen/ $\text{cm}^2$ ,  $n$  the number of oxygen atoms per  $\mu\text{g}$  of oxygen,  $\mu_a$  the mass absorption coefficient of aluminum oxide for  $O_K$  in  $\text{cm}^2/\mu\text{g}$  oxygen,  $\sigma$  the  $O_K$  production cross section in  $\text{cm}^2/\text{oxygen atom}$ , and  $E(x)$  the proton energy after traversing  $x$   $\mu\text{g}$  oxygen/ $\text{cm}^2$ . For small  $T$ , Eq. (2) reduces to

$$\lim_{T \rightarrow 0} I(E_0, T) = n\sigma(E_0)T. \quad (3)$$

Equation (2) can be transformed into a function of proton energy through the stopping power  $S(E) = -dE/dx$ . In particular, as  $T$  approaches and exceeds the proton range,  $E(T)$  approaches zero, and the yield is

$$\lim_{T \rightarrow \infty} I(E_0, T) = I_\infty(E_0) = n \int_0^{E_0} dE \frac{\sigma(E)}{S(E)} \exp\left(-\mu_a \int_E^{E_0} \frac{dE'}{S(E')}\right). \quad (4)$$

Differentiating Eq. (4) with respect to  $E_0$  gives the stopping power

$$S(E_0) = \left(\frac{dI_\infty(E_0)}{dE_0}\right)^{-1} [n\sigma(E_0) - \mu_a I_\infty(E_0)]. \quad (5)$$

## Results and Discussion

The  $O_K$  yield from eight electropolished and anodized aluminum targets bombarded by 20- to 100-keV protons was measured. The thickness of the oxide layer varied from 1 to 67  $\mu\text{g}$  O/ $\text{cm}^2$ . In addition to solid angle and x-ray window absorption corrections, the number of x-ray counts per  $\mu\text{C}$  of incident protons was corrected for proportional counter gas absorption efficiency, which was determined through observation of x-ray count rate as a function of counter pressure.

The experimental results are given in Figs. 2 and 3. The asymptotic values of the yield, which correspond to thick-target bombardment, occur at lower oxide thicknesses for reduced incident

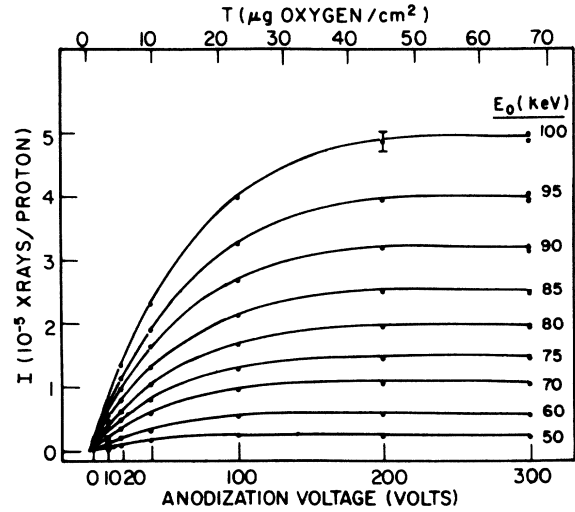


FIG. 2.  $O_K$  yields from aluminum oxide for 50- to 100-keV protons. Duplicate measurements were made at 300 V (anodization); the difference was less than 2%.

energy since the range of the proton decreases with energy. Oxide film uniformity to within  $\pm 1\%$  was noted by thick-target yield observation as the targets were rotated  $\pm 2^\circ$ . The standard deviations of the  $O_K$  measurement resulted from standard deviations of x-ray counting statistics (2% for 50- to 100-keV protons, increasing to 5% at 20 keV), integrated target current (1%), x-ray window transmission (1%), and proportional counter absorption (1%). The calculated standard deviation of the yield measurements was 3% for 50 to 100 keV and increased to 6% at 20 keV.

The x-ray yield is initially linear with oxygen surface density, and from Eq. (3) the initial slope determines the  $O_K$  production cross section as a function of proton energy. The cross section is given in Fig. 4 and in Table I. The cross section was corrected for Auger processes to give the  $K$ -

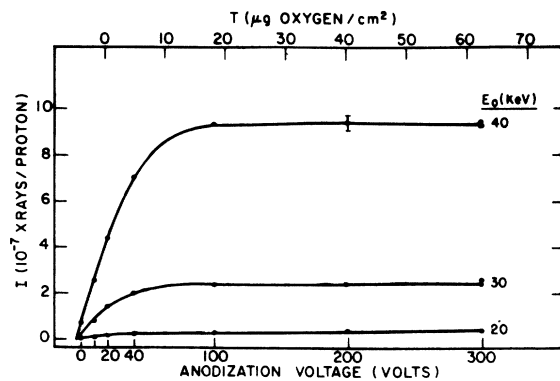


FIG. 3.  $O_K$  yields from aluminum oxide for 20- to 40-keV protons. Duplicate measurements were made at 300 V (anodization); the difference was less than 2%.

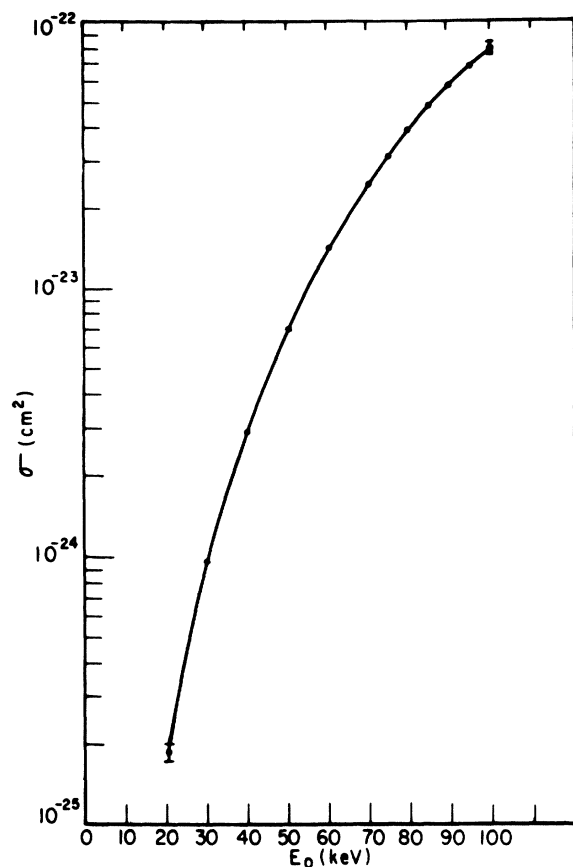


FIG. 4.  $O_K$  production cross section. The standard deviation is 5% for the 50- to 100-keV energy range and increases to 7% at 20 keV.

shell ionization cross section  $\sigma_K$  through the relationship

$$\sigma_K = \sigma / \omega_K, \quad (6)$$

where  $\omega_K$  is the fluorescence yield. Similarly, the previously measured x-ray production cross sections for the  $K$  shells of C, Mg, and Al<sup>2</sup> were converted to ionization cross sections. (The C x-ray production cross section given in Ref. 2 was based on an estimate of the stopping power. Recent measurements of the stopping power for low-energy protons in C,<sup>6</sup> permitted a more accurate calculation of this cross section.) Fluorescence-yield values were chosen by interpolation of the data given in Fink *et al.*<sup>7</sup>: C ( $7.0 \times 10^{-4}$ ), O ( $2.8 \times 10^{-3}$ ), Mg ( $2.1 \times 10^{-2}$ ), and Al ( $2.9 \times 10^{-2}$ ). The ionization cross sections are compared with the universal curve predicted on the basis of the Born approximation<sup>1</sup> in Fig. 5. Probable error of  $\pm 50\%$  is assigned to these cross sections due, primarily, to similar uncertainty in the values of  $\omega_K$ . The results for O join smoothly with the Mg and Al results, giving a composite curve which is in good

TABLE I. Interpolated values of the  $O_K$  yield from thick-target aluminum oxide,  $I_\infty(E_0)$ , and the  $O_K$  production cross section,  $\sigma(E_0)$ , where  $E_0$  is proton energy.

$E_0$ (keV)	$I_\infty(E_0)$ (x rays/proton)	$\sigma(E_0)$ (cm <sup>2</sup> )
100	$4.85 \times 10^{-5}$	$7.90 \times 10^{-23}$
95	$4.00 \times 10^{-5}$	$6.70 \times 10^{-23}$
90	$3.15 \times 10^{-5}$	$5.70 \times 10^{-23}$
85	$2.53 \times 10^{-5}$	$4.75 \times 10^{-23}$
80	$1.98 \times 10^{-5}$	$3.86 \times 10^{-23}$
75	$1.52 \times 10^{-5}$	$3.10 \times 10^{-23}$
70	$1.14 \times 10^{-5}$	$2.44 \times 10^{-23}$
65	$8.50 \times 10^{-6}$	$1.88 \times 10^{-23}$
60	$5.95 \times 10^{-6}$	$1.40 \times 10^{-23}$
55	$4.10 \times 10^{-6}$	$1.01 \times 10^{-23}$
50	$2.65 \times 10^{-6}$	$7.00 \times 10^{-24}$
45	$1.65 \times 10^{-6}$	$4.70 \times 10^{-24}$
40	$9.40 \times 10^{-7}$	$2.90 \times 10^{-24}$
35	$5.20 \times 10^{-7}$	$1.72 \times 10^{-24}$
30	$2.50 \times 10^{-7}$	$9.40 \times 10^{-25}$
25	$1.08 \times 10^{-7}$	$4.60 \times 10^{-25}$
20	$3.50 \times 10^{-8}$	$1.86 \times 10^{-25}$

agreement with the theoretical curve near the peak but departs from theory as  $\eta_K/\theta_K^2$  decreases.<sup>8</sup> The C results also agree with theoretical predictions near the peak but fall off even faster than the composite curve. The departure of experiment from theory as  $\eta_K/\theta_K^2$  decreases has been noted earlier<sup>2</sup> and apparently reflects a gradual decrease in the accuracy of the assumptions underlying the Born approximation. Nevertheless, the continuity of the composite curve tends to confirm the universality of the parameters,  $\theta_K Z_K^4 \sigma_K$  and  $\eta_K/\theta_K^2$ .

The thick-target  $O_K$  yield,  $I_\infty(E_0)$ , is taken from the asymptotic values of the curves in Figs. 2 and 3 and is given in Table I. The derivative ( $dI_\infty/dE_0$ )( $E_0$ ), when used in conjunction with Eq. (5), yields the stopping power,  $S(E_0)$ , shown in Fig. 6. The agreement of the present results with previous work is within experimental error; however, the present data has maxima at 65 and 90 keV, which are not apparent in the calculation, based on previous work. It should be noted that the reported stopping power for aluminum does have a pronounced peak at 70 keV, and the reported oxygen stopping power has a shallow peak at 90 keV. These peaks are in approximate agreement with those presented in the present data.

Since the cross section for x-ray production and the stopping power are determined from the initial slope,

$$\left( \frac{\partial I(E_0, T)}{\partial T} \right)_{T=0},$$

and the asymptotic value,  $I_\infty(E_0)$ , the validity of

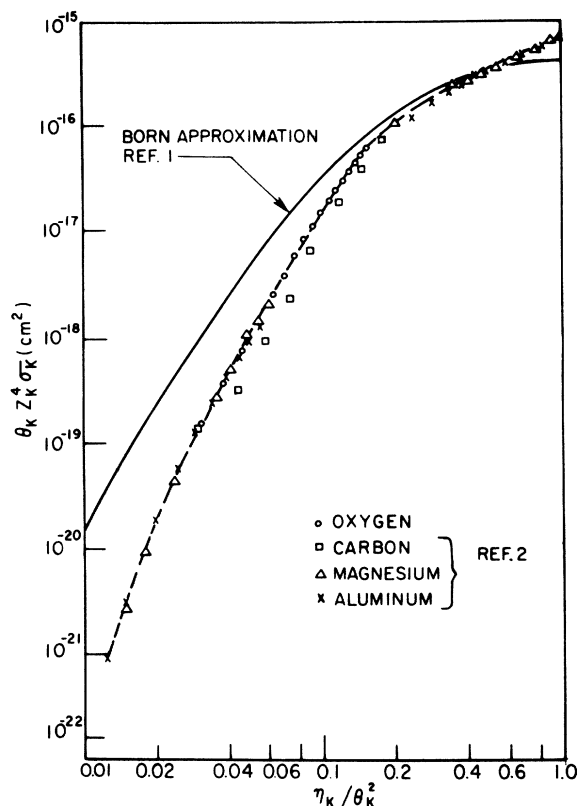


FIG. 5. Comparison of experimental  $K$ -shell ionization cross sections with the universal curve predicted in Ref. 1. The screening constant  $\theta_K$  was calculated from Walske<sup>8</sup>: C(0.64), O(0.66), Mg(0.70), and Al(0.71). The effective atomic number  $Z_K$  is equal to  $Z - 0.3$ , where  $Z$  is the atomic number of the element considered, and reduced energy variable  $\eta_K / \theta_K^2$  is  $(m/M)(E/Z_K^2 \text{ Ry})$ . The quantity  $(m/M)$  is the ratio of electron to proton masses.

Eq. (2) can be tested by comparing the results of numerical integration with the experimental data in the mid thickness range. As shown in Fig. 7, all data agree with the numerical result to within 3%, thereby suggesting that the assumptions upon which Eq. (2) is based are accurate.

An additional, thick aluminum oxide target was investigated for radiation damage effects. The x-ray yield for 100-keV proton bombardment was constant to  $\pm 1\%$  for bombardment less than  $6 \times 10^{16}$  protons/cm<sup>2</sup>. At greater integrated current density, the x-ray yield decreased 1% and decreased by 2% at  $1.4 \times 10^{17}$  protons/cm<sup>2</sup>. Primak and Luthra<sup>9</sup> have observed the onset of blistering of magnesium oxide bombarded by 140-keV protons at  $6 \times 10^{17}$  protons/cm<sup>2</sup>. Our reductions may have been caused by a similar effect. Since the targets used for the  $O_K$  measurements were bombarded by a total of  $5 \times 10^{16}$  protons/cm<sup>2</sup>, where 40% of this total was accumulated during the last mea-

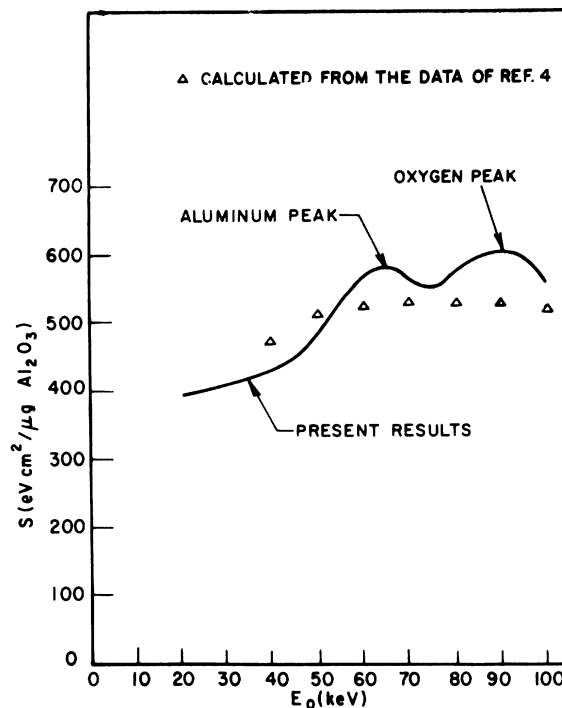


FIG. 6. Stopping power in  $\text{Al}_2\text{O}_3$ , calculated as shown in Eq. (5). The mass absorption coefficient  $\mu_a$  was taken equal to  $7.7 \times 10^{-3} \text{ cm}^2/\mu\text{g O}$ , and was determined from x-ray transmission through aluminum oxide windows. The standard deviation of the stopping power is 7% from 50 to 100 keV and increases to 10% at 20 keV. The increased error, as compared with error in x-ray yield, was primarily due to an estimated 2.5% error in converting anodization voltage to oxygen surface density. Also shown is the calculated stopping power based on the data of Ref. 4.

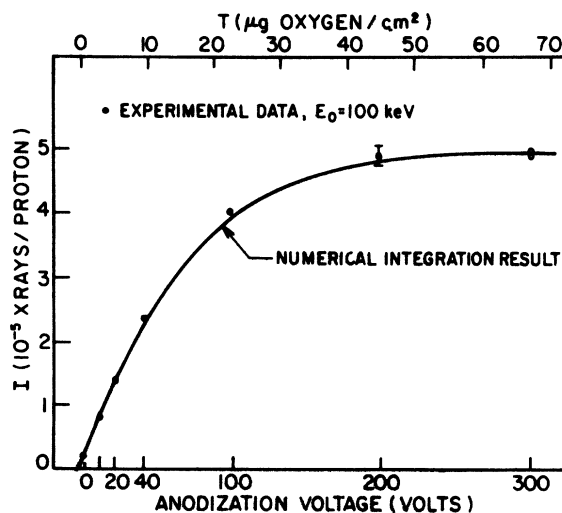


FIG. 7. Comparison of measured and calculated  $O_K$  yield in aluminum oxide films as a function of the film thickness. The incident energy of the proton is 100 keV.

surement at 20 keV, our total integrated current density was less than that at which a 1% change in yield was observed.

#### ACKNOWLEDGMENT

The authors express their gratitude to D. L.

Potter, R. D. Worley, N. T. Olson, R. G. Musket, and W. Siekhaus for many helpful suggestions. Fellowships from the National Science Foundation and the Atomic Energy Commission through the Oak Ridge Associated Universities are gratefully acknowledged (RRH and FWR).

\*This work was partially supported by the NASA Lewis Research Center.

†Present address: Hughes Research Laboratories, Malibu, California.

<sup>1</sup>E. Merzbacher and H. W. Lewis, *Encyclopedia of Physics*, edited by S. Flügge (Springer-Verlag, Berlin, 1958).

<sup>2</sup>J. M. Khan, D. L. Potter, and R. D. Worley, *Phys. Rev.* **139**, 1735 (1965).

<sup>3</sup>S. K. Allison and S. D. Warshaw, *Rev. Mod. Phys.*

**25**, 779 (1953).

<sup>4</sup>L. C. Northcliffe, *Ann. Rev. Nucl. Sci.* **13**, 67 (1963).

<sup>5</sup>R. R. Hart, N. T. Olson, Harold P. Smith, Jr., and J. M. Khan, *J. Appl. Phys.* **39**, 5538 (1968).

<sup>6</sup>J. H. Ormrod and H. E. Duckworth, *Can. J. Phys.* **41**, 1424 (1963).

<sup>7</sup>R. W. Fink, R. C. Jopson, Hans Mark, and C. D. Swift, *Rev. Mod. Phys.* **38**, 513 (1966).

<sup>8</sup>M. C. Walske, *Phys. Rev.* **101**, 940 (1956).

<sup>9</sup>W. Primak and J. Luthra, *J. Appl. Phys.* **37**, 2287 (1966).

## Radiative Decay Rates of Vacancies in the *K* and *L* Shells\*

James H. Scofield

*Lawrence Radiation Laboratory, University of California, Livermore, California 94550*

(Received 6 December 1968)

A calculation is made of the rates of emission of x rays in the filling of vacancies in the *K* and *L* shells. The total radiative decay rates and the rates of emission of a number of x-ray lines are presented for a range of elements. The atomic electrons are taken to be in single-particle states in a central potential given by the relativistic Hartree-Slater theory. All multipoles of the radiation field and all transitions from occupied states of the atom are included. The electrons are treated relativistically and the effect of retardation is included.

### INTRODUCTION

A vacancy in one of the levels of an atom may be filled by an electron from a higher level accompanied by the ejection of either a second electron or an x ray. This paper gives the results of a calculation of the rate of decay of vacancies in the *K* and *L* shells accompanied by the radiation of x rays. In the calculation, the electrons are treated relativistically and the effect of retardation is included. The electrons are treated as moving independently with their mutual interactions accounted for by a central potential. The potential used is one given by the Hartree-Slater theory.

Relativistic calculations of the radiative transition rates have previously been carried out by

Massey and Burhop,<sup>1</sup> Laskar,<sup>2</sup> Payne and Levinger,<sup>3</sup> Asaad,<sup>4</sup> Taylor and Payne,<sup>5</sup> and Babushkin.<sup>6</sup> All of these calculations except Asaad's are based on the Coulomb potential. Massey and Burhop, Laskar, and Babushkin introduced an effective nuclear charge to account for the screening of the nucleus by the electrons. Asaad's calculation is based on a more realistic potential obtained from a self-consistent field calculation. The calculations of Massey and Burhop, Laskar, and Asaad do not include the effect of retardation; i. e., they assume the x ray's wavelength is much greater than the atomic dimensions. The inclusion of retardation is incorrect in the work of Payne and Levinger and Taylor and Payne. Babushkin